

We previously proposed a tight-binding band model with full f-electron characters on Ce with spin-orbit (s.o.) interaction and the crystal electric field (CEF); we also proposed a simplified A_u top-most valence band composed of p states on X_{12} clusters.¹¹⁾ The calculated optical conductivity successfully explained the temperature dependence of the mid-infrared (IR) peak and the filling-up of the gap with increasing temperature by including strong correlation effects. However, we assumed a finite band gap in the previous work to focus on the temperature dependence of the (pseudo-)gap structures. Further, the band calculation yielded a finite gap.⁵⁾ It is now clear that $CeRu_4Sb_{12}$ is a metal at the ground state, perhaps a semimetal;³⁾ hence, we improved our model with a slight simplification and calculated the transport properties in the present paper.

In $CeRu_4Sb_{12}$, the resistivity shows a large peak at 80 K after the subtraction of the data of the La-counterpart. The Seebeck coefficient is positive and also shows a large peak at nearly the same temperature.^{2,3,12)} Non-Fermi-liquid (NFL)-like behaviors are found at very low temperatures below several Kelvin;^{2,12)} however, it is beyond the scope of this paper.

In order to explain all these features except NFL, we propose a simplified tight-binding model, which captures the essential features of the band calculation. Using this model and introducing the correlation effect within the framework of the dynamical mean field approximation and iterative perturbation theory,¹⁵⁾ the temperature dependences of the optical conductivity, resistivity and Seebeck coefficient are calculated; these can explain the experiments rather well. A theoretical understanding of the transport properties of the skutterudite compounds is very important since they have attracted considerable interest due to its high potential for application as a good new thermoelectric device.^{13,14)}

The basic crystal structure of filled skutterudites is the body-centered cubic (bcc) lattice composed of the X_{12} clusters filled by R in the center. The f orbitals of rare-earth atoms strongly hybridize with the p orbitals on X_{12} clusters close the Fermi level. The X_{12} cluster has the T_h symmetry, but its effect on the $J = 5/2$ f^1 state in Ce is the same as that of O_h . Therefore, we use the notation for O_h in the following sections.

The present band model consists of a single wide band (called c-band hereafter):

$$\begin{aligned} \varepsilon_{\mathbf{k}}^c &= t_1 \cos \frac{k_x a}{2} \cos \frac{k_y a}{2} \cos \frac{k_z a}{2} \\ &\quad + t_2 (\cos k_x a + \cos k_y a + \cos k_z a) \end{aligned} \quad (1)$$

with the nearest and the next-nearest neighbor hopping parameters on the bcc lattice, which represents the top-most p band of X_{12} clusters. The lattice constant a is set as unity in the following. For f-electrons, the neutron scattering experiment cannot resolve the CEF for the moment.¹⁶⁾ Here, we assume that the the ground state of f-electron is Γ_7 doublet as in $CeOs_4Sb_{12}$,¹⁷⁾ and take the doubly degenerate f-band; however, since CEF is not well separated, it is possible that the 6-fold $J = 5/2$ states could be a better starting model. We neglect this problem and assume the simplest

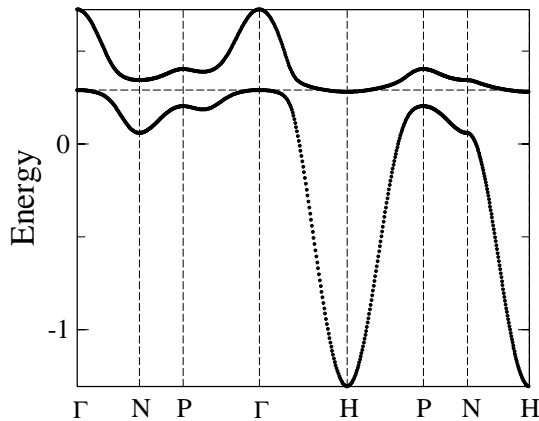


Fig. 1. The model band structure of CeRu₄Sb₁₂ calculated with the parameters $t_1 = 1.0$, $t_2 = 0.1$, $\alpha = 0.02$, $E_f = 0.3$ and $V = 0.1$ is shown. The dotted line represents the Fermi level.

model; the degeneracy may only quantitatively change the following results. Then, we assume the following simple f-band: $\epsilon_{\mathbf{k}}^f = E_f + \alpha\epsilon_{\mathbf{k}}^c$, where α is a small factor representing the width of the f-band dispersion. This may be a reasonable choice since both X₁₂ and R occupy the same bcc sites. These two c and f bands hybridize with each other.

Then, the Hamiltonian is given by

$$\begin{aligned}
 H &= \sum_{\mathbf{k}\sigma} \epsilon_{\mathbf{k}}^c c_{\mathbf{k}\sigma}^\dagger c_{\mathbf{k}\sigma} + \sum_{\mathbf{k}\sigma} \epsilon_{\mathbf{k}}^f f_{\mathbf{k}\sigma}^\dagger f_{\mathbf{k}\sigma} \\
 &+ \sum_{\mathbf{k}\sigma} \left(V c_{\mathbf{k}\sigma}^\dagger f_{\mathbf{k}\sigma} + h.c \right) + U \sum_i n_{i\uparrow}^f n_{i\downarrow}^f,
 \end{aligned} \tag{2}$$

where $c_{\mathbf{k}\sigma}^\dagger$ ($f_{\mathbf{k}\sigma}^\dagger$) creates a c (f)-electron with wave vector \mathbf{k} and spin σ (representing Γ_7 doublet), and $n_{i\sigma}^f = f_{i\sigma}^\dagger f_{i\sigma}$ with the site index i . V is the hybridization between the conduction and f-electrons, and its \mathbf{k} -dependence is neglected. These choices in our model band considerably facilitate the calculations of the strong correlation effects, which will be seen later. Actually, of course, the f-dispersion is created through the X₁₂ clusters, so that it must be self-consistently determined with $\epsilon_{\mathbf{k}}^c$ and the hybridization $V_{\mathbf{k}}$. U is the Coulomb repulsion among f electrons. $V_{\mathbf{k}}$ depends on \mathbf{k} since Γ_7 has an anisotropic shape; however, we neglect the \mathbf{k} -dependence and set $V_{\mathbf{k}} = V$ to facilitate the calculation in the following sections.

Without Coulomb interaction, the diagonalized energy dispersions become $E_{\mathbf{k}}^\pm = [\epsilon_{\mathbf{k}}^c + \epsilon_{\mathbf{k}}^f \pm \{(\epsilon_{\mathbf{k}}^c - \epsilon_{\mathbf{k}}^f)^2 + 4V^2\}^{1/2}]/2$, which are the so-called hybridized bands; however, since $\epsilon_{\mathbf{k}}^f$ has a finite dispersion, the two bands can have a finite overlap if α is not too small.

Considering the empirical trend of the lattice constant and the energy gap of Ce skutterudites, CeRu₄Sb₁₂ must be a semimetal.¹⁾ Our assumed band structure with $t_1 = 1.0$, $t_2 = 0.1$, $\alpha = 0.02$, $E_f = 0.3$ and $V = 0.1$ is shown in Fig. 1, which has a semi-metallic character: the top of the lower band (Γ point) and the bottom of the upper band (H point) slightly touch the Fermi level, and overlap by about 0.03. Although our band structure is quite simplified, Fig. 1 represents the

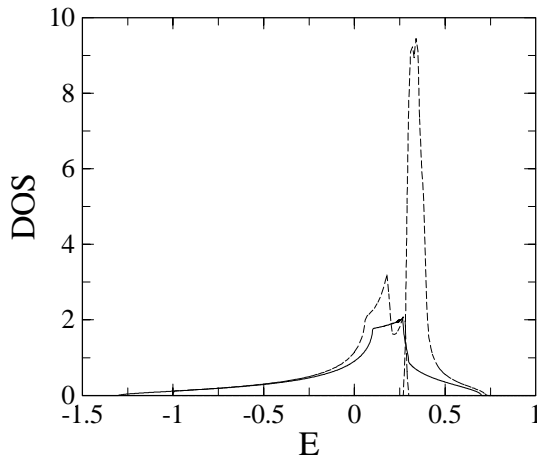


Fig. 2. The density of states $\rho_c(\varepsilon)$ for $\varepsilon_{\mathbf{k}}^c$ (solid line) and those for $E_{\mathbf{k}}^{\pm}$ (dotted lines) are shown.

low-energy structure of the band calculation for $\text{CeRu}_4\text{Sb}_{12}$ ¹⁸⁾ rather well. The density of states (DOS) $\rho_c(\varepsilon)$ for $\varepsilon_{\mathbf{k}}^c$ and those for $E_{\mathbf{k}}^{\pm}$ are shown in Fig. 2.

For treating the correlation effects, we use the dynamical mean-field theory and the iterative perturbation theory,¹⁵⁾ which is a second-order perturbation theory modified so that the weak and strong correlation limits are interpolated. Because we choose $\varepsilon_{\mathbf{k}}^f = E_f + \alpha\varepsilon_{\mathbf{k}}^c$ and V independent of \mathbf{k} , the \mathbf{k} -summation is converted into a single energy integration on $\varepsilon_{\mathbf{k}}^c$ with the density of states for this band, $\rho_c(\varepsilon)$. Therefore, the \mathbf{k} -summation over the Brillouine zone is necessary only once at the beginning and for the calculation of the dynamical conductivity given by²⁰⁾

$$\begin{aligned} \text{Re}\sigma(\omega) &= 2\pi e^2 \bar{v}_{cx}^2 \frac{1}{N} \sum_{\mathbf{k}} \int d\varepsilon \frac{f(\varepsilon) - f(\varepsilon + \omega)}{\omega} \\ &\times \left[\rho_{\mathbf{k}}^c(\varepsilon) \rho_{\mathbf{k}}^c(\varepsilon + \omega) + \alpha \rho_{\mathbf{k}}^{cf}(\varepsilon) \rho_{\mathbf{k}}^{cf}(\varepsilon + \omega) \right. \\ &\quad \left. + \alpha^2 \rho_{\mathbf{k}}^f(\varepsilon) \rho_{\mathbf{k}}^f(\varepsilon + \omega) \right]. \end{aligned} \quad (3)$$

Here, we neglected the vertex correction and replaced the velocity matrix elements by an average \bar{v}_{cx}^2 except its scaling factor α . $f(\varepsilon)$ is the Fermi function and $\rho_{\mathbf{k}}^{\gamma}(\varepsilon) = (-1/\pi)\text{Im}G_{\mathbf{k}}^{\gamma}(\varepsilon + i\delta)$ ($\gamma = c$ or f or cf) with the Green functions

$$G_{\mathbf{k}}^c(\varepsilon) = \frac{1}{\varepsilon - \varepsilon_{\mathbf{k}}^c - \frac{V^2}{\varepsilon - \varepsilon_{\mathbf{k}}^f - \Sigma_f(\varepsilon)}}, \quad (4)$$

$$G_{\mathbf{k}}^{cf}(\varepsilon) = \frac{V}{(\varepsilon - \varepsilon_{\mathbf{k}}^c)(\varepsilon - \varepsilon_{\mathbf{k}}^f - \Sigma_f(\varepsilon)) - V^2}, \quad (5)$$

$$G_{\mathbf{k}}^f(\varepsilon) = \frac{1}{\varepsilon - \varepsilon_{\mathbf{k}}^f - \Sigma_f(\varepsilon) - \frac{V^2}{\varepsilon - \varepsilon_{\mathbf{k}}^c}}. \quad (6)$$

When the imaginary parts of the self-energy and α are small, $\text{Re}\sigma(\omega)$ are dominated by the

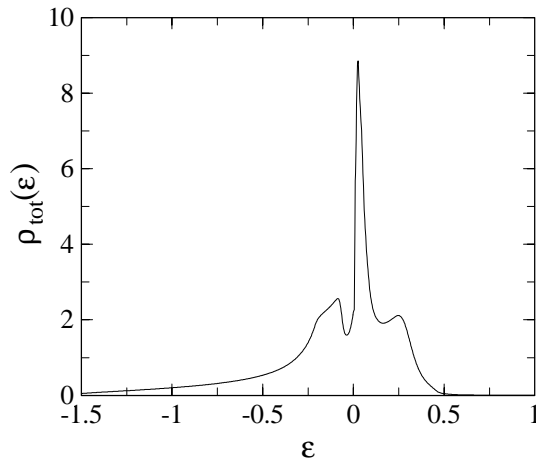


Fig. 3. The total quasi-particle density of states for $U = 0.3$ and $T = 0$ is shown. The origin of the energy is shifted to the Fermi level.

current carried by the c-electrons and can be approximated by²¹⁾

$$\begin{aligned} \text{Re}\sigma(\omega) &\simeq 2\pi e^2 \bar{v}^2 \sum_{\mathbf{k}} \frac{f(\varepsilon_{\mathbf{k}}^c) - f(\varepsilon_{\mathbf{k}}^c + \omega)}{\omega} \\ &\times \text{Im} \frac{1}{\omega + \Sigma_c^R(\varepsilon_{\mathbf{k}}^c, \mathbf{k}) - \Sigma_c^A(\varepsilon_{\mathbf{k}}^c, \mathbf{k})}, \end{aligned} \quad (7)$$

which is not a bad approximation. Here,

$$\Sigma_c(\varepsilon, \mathbf{k}) \equiv \frac{V^2}{\varepsilon - \varepsilon_{\mathbf{k}}^f - \Sigma_f(\varepsilon)}, \quad (8)$$

and R (A) denotes the retarded (advanced) function.

The resistivity $\rho(T)$ and the Seebeck coefficient $S(T)$ ²²⁻²⁴⁾ for correlated systems are given by

$$1/\rho(T) = 2e^2 \int d\varepsilon L(\varepsilon) \left(-\frac{\partial f}{\partial \varepsilon} \right), \quad (9)$$

$$\begin{aligned} S(T) &= -\frac{1}{eT} \int d\varepsilon L(\varepsilon) (\varepsilon - \mu) \left(-\frac{\partial f}{\partial \varepsilon} \right) \\ &/ \int d\varepsilon L(\varepsilon) \left(-\frac{\partial f}{\partial \varepsilon} \right), \end{aligned} \quad (10)$$

where $L(\varepsilon) \equiv (\pi N)^{-1} \sum_{\mathbf{k}} (v_{\mathbf{k}x})^2 [\text{Im} G_{\mathbf{k}}^c(\varepsilon, \mathbf{k})]^2$ when the c-electron dominates and the vertex corrections can be neglected. It can be further approximated by $L(\varepsilon) \simeq \rho_c(\varepsilon) \bar{v}_{cx}^2 \tau_c(\varepsilon)$ similar to eq.(7) with the following relaxation time of c-electrons: $\tau_c(\varepsilon_{\mathbf{k}}^c)^{-1} \simeq -2\text{Im}\Sigma_c(\varepsilon_{\mathbf{k}}^c, \mathbf{k})$. Both approximations yield similar results, as will be shown below.

We numerically solve the f-electron self-energy $\Sigma_f(\varepsilon)$ for $U = 0.3$ by iteration and calculate the above mentioned quantities. The \mathbf{k} -summations are performed over 400^3 mesh points in the $1/8$ of the extended cubic Brillouin zone. Because of the correlation effects, the quasi-particle DOS becomes temperature dependent, and the sharp Kondo peak is formed on the Fermi level at

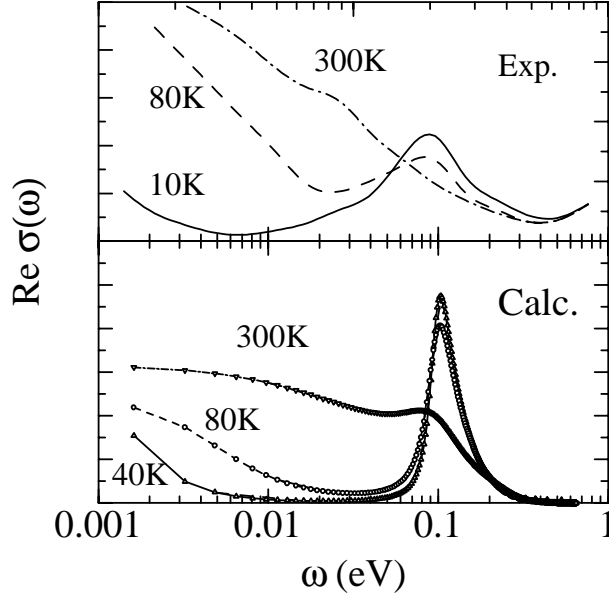


Fig. 4. The experimental⁶⁾ and theoretical results for the dynamical conductivity for various temperatures are shown.

low temperatures in addition to the upper Hubbard peak (Fig.3). The appearance of the Kondo peak enhances the temperature dependence of the physical quantities compared to the rigid band calculation.

By choosing the scale as $t_1 = 7000$ K, the calculated optical conductivity (by the correct formula, eq.(3), but using only the cc-part) in Fig. 4 shows a mid-IR peak at 0.1 eV in accordance with the experiment, but the width is narrower. There is a large pseudogap below the mid-IR peak that is the result of the direct (\mathbf{k} -conserving) interband transition; however, a Drude peak at low temperatures and frequencies since it is a semimetal. The main discrepancy is that the experimental spectrum at the lowest temperature has a long tail below the mid-IR peak, which may be due to the indirect transitions, as was pointed out recently by Okamura, et al. and the present author for the Kondo insulator YbB_{12} .^{8,9,11)} The temperature-dependence is weaker than the experiments; however, the pseudogap of the order of 0.1 eV is filled up already at $T = 300$ K, which is due to the many-body effect.^{9,11)} Despite some discrepancies, the overall structures and temperature-dependences are rather well reproduced by the present simple model.

The resistivity and Seebeck coefficient with and without the relaxation approximation are compared with the experimental values in Figs. 5 and 6. The calculated peak position agrees with the experimental value in the case of Seebeck coefficient, but it is twice as high in the resistivity. Nevertheless, our results reproduce the global features rather well, except the strange steep rise of $S(T)$ at very low temperatures and the shoulder at 20 K. The difference in $\rho(T)$ at low temperatures may be due to the residual resistivity.

We tried to fit all these data by the present model by changing the band parameters and U ;

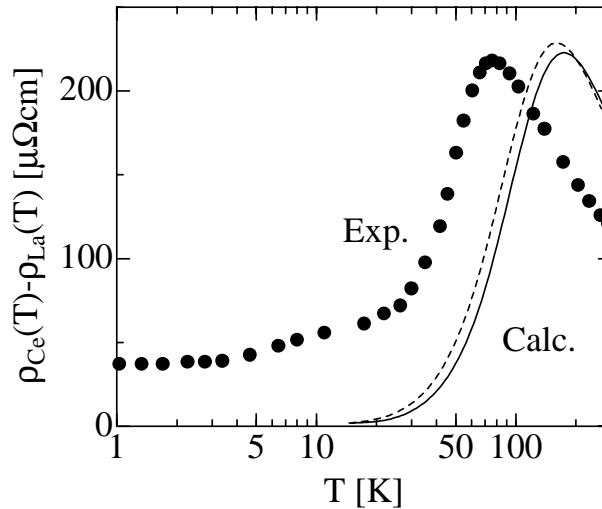


Fig. 5. The calculated resistivity (the broken line by the relaxation time approximation) compared with the experimental value is shown. (The data of the corresponding La-compound is subtracted from the experimental data.³⁾)

however, the present ones are the best. The remaining discrepancies may be due to the oversimplification of the present band model, the improvement of which is left for a future study.

In summary, we have constructed an effective tight-binding model (periodic Anderson model with dispersive f-band) to describe the low energy state of $\text{CeRu}_4\text{Sb}_{12}$, and calculated the optical conductivity, resistivity and Seebeck coefficient, taking into account the Coulomb interaction between f-electrons via the dynamical mean-field approximation and the iterative perturbation theory. The results can explain the experimental data semi-quantitatively. Improvement of the model and the consideration of the non-Fermi-liquid-like behaviors found at low temperatures remain to be done in the future.

We would like to thank Professors H. Okamura, H. Sato and H. Harima for useful informations and discussions. This work was supported by The Grant-in-Aid from the Ministry of Education, Culture, Sports, Science and Technology: Evolution of New Quantum Phenomena Realized in the Filled Skutterudite Structure, No. 16037204.

- 1) H. Sugawara, S. Osaki, M. Kobayashi, T. Namiki, S. R. Saha, Y. Aoki and H. Sato: *Phys. Rev. B* **71** (2005) 125127.
- 2) E. D. Bauer, A. Slebarski, R. P. Dickey, E. J. Freeman, C. Sirvent, V. S. Zapf, N. R. Dilly and M. B. Maple: *J. Phys.: Condens. Matter* **13** (2001) 5183.
- 3) K. Abe, H. Sato, T. D. Matsuda, T. Namiki, H. Sugawara and Y. Aoki: *J. Phys.: Condens. Matter* **14** (2002) 11757.
- 4) N. Kurita, M. Hedo, Y. Uwatoko, M. Kobayashi, H. Sugawara, H. Sato and N. Móri: *J. Magn. Magn. Mater.* **272-276** (2004) e81.
- 5) H. Harima and K. Takegahara: *J. Phys.: Condens. Matter* **15** (2003) S2081.
- 6) S. V. Dordevic, D. N. Basov, N. R. Dilley, E. D. Bauer and M. B. Maple: *Phys. Rev. Lett.* **86** (2001) 684.
- 7) M. Matsunami, H. Okamura, T. Namba, H. Sugawara and H. Sato: *J. Magn. Magn. Mater.* **272-276** (2004) e41.
- 8) H. Okamura, T. Michizawa, T. Namba, S. Kimura, F. Iga and T. Takabatake: *J. Phys. Soc. Jpn.* **74** (2005) 1954.

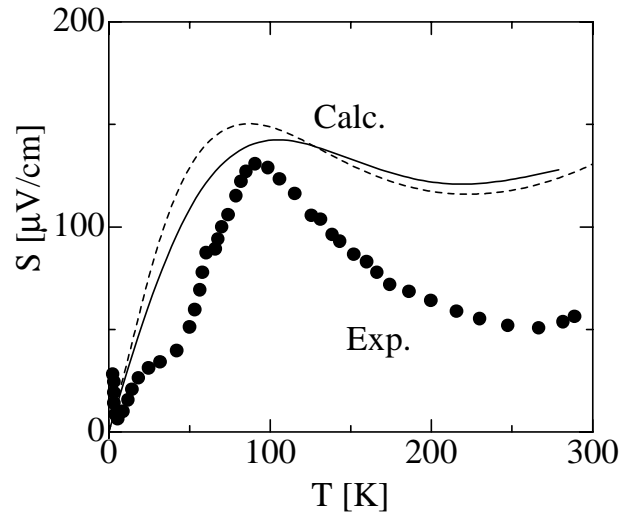


Fig. 6. The calculation for the Seebeck coefficient (the broken line by the relaxation time approximation) is compared with the experiment.³⁾

- 9) T. Saso: J. Phys. Soc. Jpn. **73** (2004) 2894.
- 10) Y. Imai, K. Sakurazawa and T. Saso: J. Phys. Soc. Jpn. **75** No.3 (2006) (in press).
- 11) T. Mutou and T. Saso: J. Phys. Soc. Jpn. **73** (2004) 2900-2905.
- 12) N. Takeda and M. Ishikawa: J. Phys. Soc. Jpn. **69** (2000) 868.
- 13) B. C. Sales, D. Mandrus and R. K. Willams: Science **272** (1996) 1325.
- 14) B. C. Sales, D. Mandrus, B. C. Chakoumakos, V. Keppens and J. R. Thompson: Phys. Rev. B **56** (1996) 15081.
- 15) H. Kajueter and G. Kotliar: Phys. Rev. Lett. **77** (1996) 131.
- 16) D. T. Adroja, J.-G. Park, K. A. McEwen, N. Takeda, M. Ishikawa and J.-Y. So: Phys. Rev. B **68** (2003) 094425.
- 17) E. D. Bauer, A. Slebarski, E. J. Freeman, C. Sirvent and M. B. Maple: J. Phys.: Condens. Matter **13** (2001) 4495.
- 18) H. Harima: private communication.
- 19) T. Saso and H. Harima: J. Phy. Soc. Jpn. **72** (2003) 1131.
- 20) T. Mutou: Phys. Rev. B **64** (2001) 245102.
- 21) B. P. Stojkovic and D. Pines: Phys. Rev. B **56** (1997) 11931.
- 22) M. Jonson and G. D. Mahan: Phys. Rev. B **42** (1990) 9350.
- 23) G. D. Mahan: *Solid State Physics*, eds. H. Ehrenreich and F. Spaepen, (Academic Press, 1998) Vol. **51**, p. 81.
- 24) G. D. Mahan: *Many-Particle Physics, Third Edition* (Kluwer Academic/Plenum, 2000)